

Distributed-Memory Parallel Contig Generation for *De Novo* Long-Read Genome Assembly

Giulia Guidi*

University of California, Berkeley
Lawrence Berkeley National
Laboratory
Berkeley, California, USA

Gabriel Raulet*

Lawrence Berkeley National
Laboratory
Berkeley, California, USA

Daniel Rokhsar

University of California, Berkeley
DOE Joint Genome Institute
Berkeley, California, USA

Leonid Olikier

Lawrence Berkeley National
Laboratory
Berkeley, California, USA

Katherine Yelick

University of California, Berkeley
Lawrence Berkeley National
Laboratory
Berkeley, California, USA

Aydın Buluç

University of California, Berkeley
Lawrence Berkeley National
Laboratory
Berkeley, California, USA

ABSTRACT

De novo genome assembly, i.e., rebuilding the sequence of an unknown genome from redundant and erroneous short sequences, is a key but computationally intensive step in many genomics pipelines. The exponential growth of genomic data is increasing the computational demand and requires scalable, high-performance approaches.

In this work, we present a novel distributed memory algorithm that, from a string graph representation of the genome and using sparse matrices, generates the contig set, i.e., overlapping sequences that form a map representing a region of a chromosome.

Using matrix abstraction, we mask branches in the string graph, and compute the connected component to group genomic sequences that belong to the same linear chain (i.e., contig). Then, we perform multiway number partitioning to minimize the load imbalance in local assembly, i.e., concatenation of sequences from a given contig. Based on the assignment obtained by partitioning, we compute the induce subgraph function to redistribute sequences between processes, resulting in a set of local sparse matrices. Finally, we traverse each matrix using depth-first search to concatenate sequences.

Our algorithm shows good scaling with parallel efficiency up to 80% on 128 nodes, resulting in uniform genome coverage and showing promising results in terms of assembly quality. Our contig generation algorithm localizes the assembly process to significantly reduce the amount of computation spent on this step. Our work is a step forward for efficient *de novo* long read assembly of large genomes in a distributed memory.

ACM Reference Format:

Giulia Guidi, Gabriel Raulet, Daniel Rokhsar, Leonid Olikier, Katherine Yelick, and Aydın Buluç. 2022. Distributed-Memory Parallel Contig Generation for *De Novo* Long-Read Genome Assembly. In *51st International Conference on*

*Both authors contributed equally to this research.

Permission to make digital or hard copies of part or all of this work for personal or classroom use is granted without fee provided that copies are not made or distributed for profit or commercial advantage and that copies bear this notice and the full citation on the first page. Copyrights for third-party components of this work must be honored. For all other uses, contact the owner/author(s).

ICPP '22, August 29-September 1, 2022, Bordeaux, France

© 2022 Copyright held by the owner/author(s).

ACM ISBN 978-1-4503-9733-9/22/08.

<https://doi.org/10.1145/3545008.3545050>

Parallel Processing (ICPP '22), August 29-September 1, 2022, Bordeaux, France.
ACM, New York, NY, USA, 11 pages. <https://doi.org/10.1145/3545008.3545050>

1 INTRODUCTION

Genomics is facing exponential growth in data coming from improved and cheaper instrumentation that is overwhelming conventional analytical infrastructures. It is especially true for *de novo* genome assembly [42], that is decoding the sequence of an unknown genome from redundant and erroneous short sequences. A key but computationally intensive step in many genomics pipelines.

On the one hand, large-scale parallel systems promise to overcome the computational and memory limitation of conventional shared-memory computing. On the other hand, programming such large-scale systems is challenging, especially when computation is highly irregular, as is often the case in genomics.

The advent of long-read sequencing technologies [14, 19], which yield sequences with an average length of more than 10,000 base pairs (bp), improved our ability to assemble complex genomic repeats and obtain more accurate assemblies that were not possible with short-read technologies [34, 37]. In the past, longer sequences were associated with higher error rates [27], resulting in significantly higher algorithm complexity and computational costs. Recent advances in sequencing technologies have lowered error rates, reducing the need for error correction and polishing phases, but computational costs remain high as we generate more data and reconstruct higher quality assemblies.

It is common practice to assemble long-read data according to the Overlap–Layout–Consensus (OLC) paradigm [6]. The first step (O) is to identify overlaps between reads to create an *overlap* graph. The second step (L) simplifies the overlap graph by removing redundant information and transforming it into an *string* graph. The third step (C) takes the string graph and processes it to obtain a first draft of the unknown genome, returning a contig set as output. A *contig* is a group of overlapping DNA sequences that together form a region of a chromosome. A common approach to contig generation takes the string graph as input, branching nodes in this graph are masked, and the set of linear, unbranched paths in the graph is extracted to form the contig set. This step can be followed by further polishing phases to merge and correct the contig set and to separate haplotypes.

In this paper, we build on previous work in the literature, diBELLA 2D [23, 24], and present a novel distributed-memory algorithm that generates the contig set starting from a string graph representation of the genome and using a sparse matrix abstraction. The proposed approaches are implemented in a software package called ELBA, which also includes the overlap and layout phases of diBELLA 2D, which can scale to hundreds of nodes. Each stage of the computation in ELBA is implemented for distributed memory.

The algorithm first determines the contig set starting from a string graph by masking out the branches and extracting the non-branched paths by computing connected components over the graph (i.e., a sparse matrix). Using a greedy multiway number partitioning algorithm, ELBA then determines how to redistribute sequences (i.e., rows and columns of the sparse matrix) between processes so that sequences belonging to the same contig are stored on the same processor. Once the sequences-to-processor assignment is computed, ELBA uses this information to implement the induced subgraph function that redistributes the sequences using sparse matrix abstraction so that each processor has a local sparse matrix representing the non-branching contig(s) assigned to the processor. ELBA then computes a local assembly step on each processor independently and in parallel. In doing so, it uses depth-first search to concatenate the sequences belonging to a particular contig and return the contig set. ELBA is the first distributed-memory implementation of the OLC assembly paradigm.

Our algorithm shows good scaling with parallel efficiency up to 80% on 128 nodes on a representative dataset. Our approach leads to uniform coverage of the genome and shows promising results in terms of assembly quality. Our contig generation algorithm is fast and efficient because it localizes the graph traversal problem, i.e., the practical concatenation of sequences, so that most of the computation can be performed locally without requiring fine-grained communication. Compared to related work, this approach significantly reduces the fraction of the runtime required by the entire assembly pipeline for contig generation. Our implementation is publicly available at <https://github.com/PASSIONLab/ELBA>.

2 BACKGROUND

A genome consists of one or more linear chains of DNA molecules, i.e., nucleotides or bases, represented by the alphabet $\Sigma = \{A, C, G, T\}$. Each linear chain has a direction and is paired with a second chain called its *reverse complement*, which has the opposite direction. Together they are called *strands* and wind around each other to form a double helix; this double helix is organized in three-dimensional space and forms a chromosome. Different species may have different numbers of chromosomes. On the opposite strands, A always pairs with T and C pairs with G. Given a string $v = \text{ATTCG}$, its reverse complement is $v' = \text{CGAAT}$.

The goal of *de novo* long-read genome assembly is to reconstruct an unknown genome sequence, possibly consisting of multiple chromosomes, starting from a collection of redundant, erroneous, and significantly shorter sequences called *reads*. For long-read sequencing data, this is commonly done following the OLC assembly paradigm introduced in the previous section. In this paper, we take the overlap (O) and layout (L) phases as implemented in diBELLA 2D [23, 24] and extend them to include the third (C) phase, that is contig generation. diBELLA 2D uses a k -mer-based approach and

relies on parallel sparse matrix multiplication for overlap detection and transitive reduction to obtain a string graph (i.e., the input to the contig generation algorithm described in Section 4).

diBELLA 2D sees the overlap detection step as a sparse matrix multiplication between a $|\text{sequences}|$ -by- $|k\text{-mers}|$ matrix A and its transpose A^T . The resulting matrix $C = AA^T$ is a sparse $|\text{sequences}|$ -by- $|\text{sequences}|$ that stores information about which sequences share at least one k -mer. diBELLA 2D then computes an element-wise pairwise alignment step for each non-zero in the C matrix, removing non-zeros that are below a certain alignment threshold. The result of this operation is the result matrix R , which in turn is the input for the transitive reduction phase, whose goal is to remove redundancies from the overlap graph and return a string graph in the form of a sparse matrix S .

A string graph (or matrix) is a graph $G = (V, E)$, where V is the set of sequences and E is the set of overlap *suffixes* between any two vertices. A string graph contains neither redundant edges nor redundant vertices. A redundant vertex is a read that is completely contained (i.e., aligned) within another read and whose edges therefore contain information that the containing read already has. A redundant edge or transitive edge is an edge that carries less or the same information as a parallel path in the graph and therefore can be removed without loss of information during transitive reduction.

In diBELLA 2D, so also in ELBA, the string graph is encoded as a bidirected graph, so we can encode information about both DNA strands. A *bidirected graph* [13] is one in which each edge at each end has an independent orientation (or arrow). There are three types of bidirected edges: (a) those with arrows at both ends pointing outward, (b) those with both arrows pointing inward, and (c) those with both arrows pointing in the same direction, one away from its vertex and the other toward its vertex.

Given two vertices v_i and v_j , the edge $e_{i,j}$ between them defines an overlap between the two vertices (i.e., sequences). The weight $w_{i,j}$ of the edge $e_{i,j}$ stores the *overhang length* or suffix length, i.e., the part of v_j that goes beyond the overlap between v_i and v_j , and its direction, i.e., how such sequences overlap with each other (for example, v_i and v_j could have the same strand orientation and the final portion of v_i could overlap with the initial portion of v_j).

If $G = (V, E)$ is a bidirected string graph, then a *valid walk* in G is a continuous sequence of edges where each vertex is entered by an inward head and exited by an outward head (unless it is the end of the path) or vice versa.

A contig is a collection of overlapping DNA sequences that together form a consensus region of DNA, such as a chromosome. To be considered a contig, a set of overlapping sequences must form a linear chain that is a valid walk.

3 RELATED WORK

Contig generation is an important step in any *de novo* genome assembly pipeline, regardless of the type of sequencing technology (long-read or short-read). In this section, we summarize the literature on this kernel and explain how it relates to our work.

The paradigm for assembling long-read sequencing data is composed of three main stages: finding overlapping sequences to create an overlap graph, removing redundant information to simplify the graph, and generating the contig set.

HiCanu [36] and Falcon-Unzip [12] implement similar approaches inspired by the Bogart algorithm presented by Canu [29] to generate the contig set in shared memory starting from a sparse long-read overlap graph or a string graph. The Bogart module creates an assembly graph using a variant of the *best overlap graph* strategy of Miller et al [33], where a *best* overlap is the longest overlap to a given read end excluding *contained* sequences (i.e., when all bases in one sequence are aligned to another sequence). The Bogart algorithm removes overlapping sequences from the overlap graph to include only those that are within some tolerance of the global median error rate, and recalculates the longest overlapping sequences using only that subset (i.e., a sparse overlap graph). Bogart generates the initial contig set from the maximum non-branching paths in that graph.

The Shasta assembler [40] also uses a similar procedure by creating an undirected graph where each vertex is an oriented read (i.e., each read contributes two vertices to the read graph, one in its original orientation and one in the reverse complement orientation) and an undirected edge is created between two vertices when we find an alignment between the corresponding oriented sequences. To reduce the high connectivity in the repeat regions, the Shasta assembler preserves only the k -nearest neighbor subset of the edges. The contig set is created from the linear structures of the graph.

In contrast, Hifiasm [11] generates a primary assembly based on the topological structures of the graph and the phasing relationship between the different haplotypes using a bubble-popping procedure [30]. Finally, a best overlap graph is used to deal with remaining unresolved substructures in the assembly graph.

A De Bruijn graph-based approach is common [31] for genome assembly of short-read sequencing data, but it has not been suitable for long-read data in the past because of higher error rates.

PaKman [18] is a parallel distributed memory contig generation algorithm for short-read sequencing technology. PaKman introduces a new compact data representation of the De Bruijn graph, named PaK-Graph, which uses iterative compression to fit the graph into the memory available on each node. This compression enables low-cost replication of the graph across nodes, reducing the need for communication and creating an embarrassingly parallel procedure. PaKman also introduces an algorithm to perform non-redundant contig generation, i.e., to avoid two processes traversing the same path in the graph and generating the same contig.

MetaHipMer [17, 26] and the earlier HipMer [16] are distributed-memory *de novo* metagenome and genome assembly pipelines, respectively, designed for short-read data and thus also use the De Bruijn-based approach. Both are implemented using a partitioned global address space model in either UPC [10] or UPC++ [5]. Contig generation is performed after the construction of a distributed hash table of k -mers with the left and right base extension from the input data stored with each k -mer. Each process then creates contigs by starting at a k -mer, walking left and right, appending the extension, and looking up the resulting k -mer in the hash table. These lookups often take place on remote nodes and are performed with either a remote memory operation or a remote procedure call. If a previously visited k -mer is reached during this process, the two contigs are merged. Fine-grained synchronization prevents a data race that can occur when two processes attempt to merge at the same time.

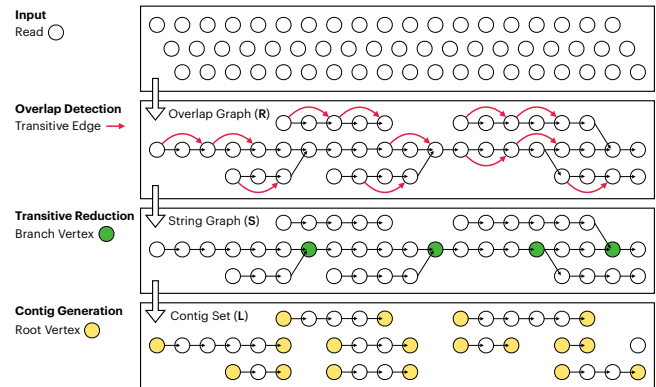


Figure 1: A high-level representation of ELBA built on diBELLA 2D [24] and extended to include contig generation, which is critical to the assembly process.

As error rates decrease for long-read data, we find in the state of the art some attempt to use a De Bruijn graph approach for this type of sequencing technology, such as the shared-memory assembler Flye [28]. Instead of generating a contig set, Flye first generates a *disjointig* set, i.e. concatenating multiple disjoint genomic sequences, and then concatenates these error-prone disjointigs into a single string (in any order), constructs an assembly graph from the resulting concatenation, uses sequences to disentangle this graph, and resolves bridged repetitive areas (which are bridged by some sequences in the repeat graph). It then uses the repeat graph to resolve unbridged repetitive areas (that are not bridged by sequences) based on the differences between repeat copies. The output is a contig set generated from the paths in this graph. Using a De Bruijn approach in conjunction with long read sequencing data leads to more complex algorithms than those commonly used in an OLC-based assembler. This makes an approach such as Flye’s unsuitable for scalable implementation on distributed memory architectures, as the access patterns are extremely fine-grained.

Regarding the use of sparse matrices and matrices in general for genomic computations, there is related work for both shared and distributed memory machines. The shared-memory software BELLA [23] is the first work to propose the use of sparse matrices in the context of *de novo* genome composition, focusing on the overlap detection phase. A sparse matrix A is used to indicate the presence of k -mers in sequences, and by multiplying by their transpose, i.e. AA^T , BELLA identifies overlapping sequences.

diBELLA 2D [24] resembles BELLA, in that it computes both overlap detection and transitive reduction over an overlap graph as distributed SpGEMM and sparse computation. PASTIS [39], similarly, computes protein homology search as distributed SpGEMM.

Besta et al. [7] present an approach, similar to BELLA, for calculating Jaccard similarity between sequences of different genomes using distributed SpGEMM. The main difference is that their software is optimized for the case where the output matrix is dense.

Algorithm 1 Parallel matrix-based computation in ELBA.

```

1: procedure ELBA
2:    $sequences \leftarrow \text{FASTAREADER}()$ 
3:    $k\text{-mers} \leftarrow \text{KMERCOUNTER}()$ 
4:    $A \leftarrow \text{GENERATEA}(sequences, k\text{-mers})$ 
5:    $A^T \leftarrow \text{TRANSPOSE}(A)$ 
6:    $C \leftarrow AA^T$  ▷ Candidate overlap matrix
7:    $C \leftarrow \text{APPLY}(C, \text{Alignment}())$  ▷ Run alignment
8:    $R \leftarrow \text{PRUNE}(C, \text{AlignmentScoreLessThan}(t))$ 
9:    $R \leftarrow \text{PRUNE}(R, \text{IsContainedRead}())$ 
10:   $S \leftarrow \text{TRANSITIVEREDUCTION}(R)$ 
11:   $cset \leftarrow \text{CONTIGGENERATION}(S)$  ▷ Algorithm 2
12:  return  $cset$ 

```

Algorithm 2 Parallel contig generation on S .

```

1: procedure CONTIGGENERATION( $S, sequences$ )
2:   $L \leftarrow \text{BRANCHREMOVAL}(S)$ 
3:   $v \leftarrow \text{CONNECTEDCOMPONENT}(L)$ 
4:   $p \leftarrow \text{GREEDYPARTITIONING}(v, P)$ 
5:   $P \leftarrow \text{INDUCEDSUBGRAPH}(L, p)$ 
6:   $cset \leftarrow \text{LOCALASSEMBLY}(P, sequences)$ 
7:  return  $cset$ 

```

4 ALGORITHM

In this section, we introduce ELBA, a parallel distributed memory algorithm designed to generate a contig set from a string graph representation of long read sequencing data.

ELBA uses sparse matrices as the core data structure throughout the computation. This abstraction leads to a flexible and modular software design, as well as high parallelization that performs well in distributed memory. To implement parallel computation over sparse matrices, we use the Combinatorial BLAS (CombBLAS) library [4], a well-known framework for implementing graph algorithms in the language of linear algebra, and use a semiring abstraction to overload the classical multiplication and addition operation as needed. ELBA is inspired by Canu’s best-overlap graph strategy [29] and improves upon the transitive reduction algorithm presented in diBELLA 2D [24] by extracting a set of high-quality, non-branching paths from the string graph.

Unlike MetaHipMer, which uses fine-grained communication at nearly every step of contig construction, ELBA localizes the graph traversal problem so that the sequences that make up a contig are stored locally at each rank, avoiding communication.

4.1 Overview

ELBA uses a highly parallelizable strategy to generate the contig set in a distributed memory environment. This means that each processor may not have access to the entire set of sequences it needs for contig generation because they are distributed among processes. Read sequences must therefore be communicated across the processor grid before contigs are generated via depth-first search.

To efficiently communicate sequences where they are needed, ELBA uses a parallel algorithm, implemented as a sparse matrix-based computation over the string matrix, to extract information

about which sequences belong to the same contig (i.e., a *linear component*) and therefore need to be sent to the same processor. A linear component of a graph is the maximal subgraph where each vertex is connected to two adjacent vertices, except for two vertices that mark the extremities of the linear chain, which are connected to a vertex. Once the membership of each sequence is known (i.e., to which contig it belongs), ELBA uses this information to achieve load balancing that ensures that each processor has similar amount of work during the local assembly process.

This is achieved by first estimating the contig sizes, i.e., the number of reads belonging to a particular contig, in parallel and then assigning approximately equal collections of contig sets to each process. Then, the sequences are redistributed among the processes using a newly implemented function that is also based on sparse matrix computation. This function generates local matrices from a distributed matrix (in our case, the string matrix) on each process according to the load-balanced assignment. ELBA then assembles the contigs whose sequence connectivity is stored in the local matrix in parallel on each processor without requiring any further communication.

Algorithm 1 summarizes the entire computation, including overlap detection and transitive reduction—lines 11-12 represent the main contribution of this work, better represented in Algorithm 2: (a) how the contig set is determined (line 2), (b) how the workload is distributed among the processes (lines 3-4), and (c) how the local assembly is performed (line 5) and the contig set is output.

4.2 Contig Set Determination

The first step in our contig generation algorithm is to determine which sequences belong to which contig based on the connectivity of the string graph.

Let us define a linear component of the graph as the maximal subgraph $L \subseteq R = (V, E)$ where (a) each vertex has either degree one or two and (b) the subgraph is connected. In a linear component there are exactly two vertices which can have degree one due to the connectedness rule. These vertices are the endpoint vertices.

Then, we define the *contig set* of R as the set of all linear chains which are not themselves subgraphs of another linear chain in R . Thus, the contig set consists of several independent collections of nodes in the bidirected string graph, where each collection is a linear sequence of unique overlapping sequences. The determination of the contig set can be done in two stages.

First we have to identify *branching vertices* that are vertices whose degree is ≥ 3 . These vertices would make it impossible to determine a unique linear chain. Therefore, our goal is to mask out such branching vertices to obtain only linear sequences of vertices. For example, consider a string graph consisting of (a) $v_1 \rightarrow v_2 \rightarrow v_3$, (b) $v_3 \rightarrow v_4 \rightarrow v_5 \rightarrow v_6$, and (c) $v_3 \rightarrow v_7 \rightarrow v_8$, the vertex v_3 is a branching vertex since its degree is equal to three, and it would not allow us to extract a linear chain, since at this point in the computation we cannot know whether the correct linear path is (i) $v_1 \rightarrow v_2 \rightarrow v_3 \rightarrow v_4 \rightarrow v_5 \rightarrow v_6$ or (ii) $v_1 \rightarrow v_2 \rightarrow v_3 \rightarrow v_7 \rightarrow v_8$. Thus, we mask out v_3 to obtain three linear sequences of vertices: (i) $v_1 \rightarrow v_2$, (ii) $v_4 \rightarrow v_5 \rightarrow v_6$, and (iii) $v_7 \rightarrow v_8$.

To identify branching vertices, we perform a summation reduction over the row dimension of the string matrix (i.e., an adjacency

matrix) and return a distributed vector \mathbf{d} whose values represent the degree of the corresponding row sequence (i.e., the index of the vector). Then we perform an element-wise selection operation on the degree vector \mathbf{d} to extract the indices (sequences) whose value is greater than or equal to 3. The result is a distributed vector \mathbf{b} whose values are the indices of the branching vertices. The branch vector \mathbf{b} is used to remove the corresponding rows and columns from the string matrix S and create a linear chain version of S that we name L (line 2, Algorithm 2). From a graph-theoretic point of view, this operation removes (i.e., sets to zero) the edges adjacent to branching vertices. The indexing of the matrix does not change, but its nonzeros do. For example, if row 10 is a branching vertex, the entire row—and column, since S is symmetric—is cleared, but row 10 is still a row in the matrix. This way we can avoid re-indexing sequences during the computation. The result is an even sparser string graph with nodes of degree 0, 1 or 2. For each contig, there are exactly two vertices of degree 1, which we call root nodes (or root vertices) and use as starting points for depth-first search and local assembly of the contig in the final stage of contig generation.

Once the string matrix is in its unbranched form L , we want to decompose it into its linear components to produce manageable independent subproblems that we can work on in parallel (i.e., local assemblies). Therefore, we use the sparse matrix based connected components (LACC) algorithm presented by Azad et al. [3] to determine the contig set. LACC is a distributed-memory implementation of the Awerbuch-Shiloach algorithm [2] using the CombBLAS library. LACC takes advantage of the sparsity of the vector to avoid processing inactive vertices. It takes as input the unbranched sparse matrix L and returns a distributed vector \mathbf{v} (line 3, Algorithm 2), which is a mapping from global sequence indices (i.e., rows and columns of S) to contig indices C_i . In the previous graph example, LACC would return $v_1, v_2 \in C_1$, $v_4, v_5, v_6 \in C_2$, and $v_7, v_8 \in C_3$.

Once we have determined which sequences belong to which contig, we estimate the size of each contig by counting how many sequences belong to it. However, since \mathbf{v} is a distributed vector, a processor may not know the full set of sequences belonging to the contig it owns. Therefore, we need to communicate this information across the processor grid. Each processor computes a local size estimate based on the vertices it owns locally for each local contig. An MPI Reduce-scatter collective operation is used to determine the global size of each contig and redistribute the sizes across the processor grid to create a distributed mapping of contig indices to their associated global sizes.

4.3 Contig Load Balancing and Communication

Previously, we determined which sequences belong to which contig and estimated the size of each contig based on the number of sequences associated with it. Using the contig size as an optimization parameter, we want to distribute the workload as evenly as possible across the processor grid.

Load Balancing Algorithm. Given a vector of contig sizes of length n and P processes, we want to find the near-optimal contig-to-processor assignment such that the amount of work estimated by the contig size that each processor has to do is similar. Our objective

and problem definition is similar to the *multiway number partitioning* optimization problem first introduced by Ronald Graham in the context of the identical-machines scheduling problem [20]. The classical application is to schedule a set of m jobs with different runtimes on k identical machines in such a way that the makespan, i.e., the elapsed time until the schedule is completed, is minimized.

In the context of contig generation, this means that given a multiset of S instances (in our case, the contig sizes), we want to partition this multiset into P subsets (the number of processes in our processor grid and must be a positive integer) such that the sums of the subsets (i.e., the sums of the contig sizes) are as similar as possible. The partitioning results in a balanced distribution of the workload for the next and final phase of the computation.

The multiway number partitioning problem is NP-hard. To overcome this limitation, in ELBA we use an approximation algorithm known in the scheduling literature as the Longest Processing Time (LPT) algorithm, whose goal is to minimize the largest subset, which belongs to a class of algorithms known as *greedy number partitioning*. The algorithm loops over the contig sizes and inserts each number into the set whose current sum of sizes is smallest. The result is a partitioning that minimizes the time processes spend waiting for the most heavily loaded process to finish assembling its contig subset. If the contig sizes were not sorted, then the runtime would be $O(n)$ and the approximation ratio would be at most $2 - 1/P$. It is possible to improve the approximation ratio to $(4P - 1)/3P$ by sorting the input vector of contig sizes [21].

The improvement in the approximation using LPT is accompanied by an increase in the runtime to $O(n \log n)$ due to sorting. However, the number of contigs n is smaller than the number of sequences by at least an order of magnitude, and the increase in runtime does not create a computational bottleneck. For the same reason, we collect the global information about contig lengths in a single processor and run the partitioning algorithm on it to avoid the unnecessary communication of small messages. The partitioning algorithm returns the vector \mathbf{p} specifying the assignment of contigs to processes (line 4, Algorithm 2)— \mathbf{p} is broadcasted to the entire processor grid so that each local process can determine where to send its local sequences and associated information.

As mentioned earlier, the problem size at this stage of the computation is often smaller than the problem size at the initial stage (i.e., overlap detection), so for some species it is possible that $n < P$. In this case, some of the processes are idle for the final phase of the computation. For the two species we use in the experimental evaluation in Section 6.2, n is equal to 6411 and 4287 and P varies from 18 to 128. In the next section, we explain how contigs are redistributed among processes based on their size.

Induced Subgraph Algorithm. Once we have determined where a contig and its sequences should be stored, we must perform the actual communication step to send the linear component information and associated sequences to the owner processor.

Communicating both the linear component information and the sequences involves the same high-level procedure of reassigning vertices representing a linear chain to their owner processor. However, the underlying data structures are fundamentally different, namely that the overlap graph is stored as a sparse matrix while

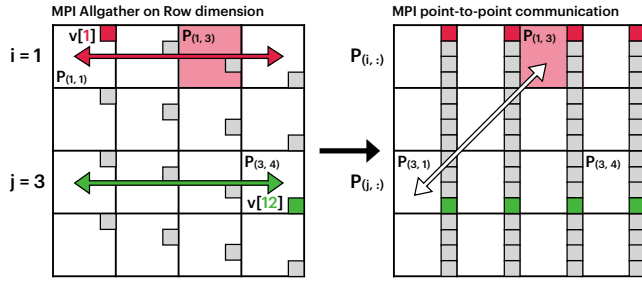


Figure 2: An example of how the induced subgraph algorithm communicates vertices across the processor grid.

the sequences are stored as distributed char arrays, and therefore require a different implementation.

Let us first focus on the communication of linear component information, i.e. the graph-like structure that stores connectivity information. We have as input the sequence-by-sequence matrix L , the resulting matrix after the transitive reduction step and from which we have cut out vertices of degree ≥ 3 . L is distributed over P processes, which are logically organized in a $\sqrt{P} \times \sqrt{P}$ grid. Let n be the number of vertices in L , where $L = (V, E)$ in the graph interpretation. From the load balancing algorithm, we have a distributed vector $v : [n] \rightarrow [P]$ such that $v[u] = P_i$ means that vertex u should belong to processor P_i .

The goal is to create an induced subgraph—or submatrix— $L^{(P_i)}$ locally on each processor P_i , i.e., a graph formed by a subset of the vertices of the original graph L and the edges connecting the vertices in this subset. Formally, we define an induced subgraph $L^{(P_i)}$ such that $L^{(P_i)} = (V^{(P_i)}, E^{(P_i)})$ with $V^{(P_i)} = \{v \in V : P_i = v[v]\}$ and $E^{(P_i)} = \{(u, v) \in E : u, v \in V^{(P_i)}\}$.

The vector v is also distributed across the $\sqrt{P} \times \sqrt{P}$ processor grid and is therefore divided into P subvectors, each of size $\approx n/P$; note that we write $v_{(i,j)}$ to denote the subvector on process $P(i, j)$. Each process is only aware of which vertices it stores to send to other processes. Therefore, we need a communication step to make each process aware of which vertices to receive. Given the way v is distributed, we can avoid an MPI_Allgather operation spanning the entire grid and instead use the square process grid to communicate v in a scalable way. That is, we perform an allgather operation over the **Row** dimension followed by point-to-point communication to access the information stored on the **Column** dimension.

More precisely, let $(u, v) \in L_{i,j}$ be any nonzero value, where $L_{i,j}$ is the local submatrix stored on processor $P(i, j)$. The goal is to determine $v[u]$ and $v[v]$. Given we know (u, v) is stored in the submatrix $L_{i,j}$, we know that $v[u]$ is stored in the row $P(i, :)$. Thus, we can access $v[u]$ by computing an MPI_Allgather operation over the processor row $P(i, :)$ and, more generally, over the **Row** dimension of S . To determine $v[v]$, we first note that if we are a diagonal processor, i.e. $i = j$, we already have access to $v[v]$ via the previous MPI_Allgather operation. If $i \neq j$, then we know that $v[v]$ is stored on the transposed processor $P(j, i)$ because we performed the allgather operation over the **Row** dimension, i.e. $P(j, :)$. Therefore, we perform a point-to-point communication between $P(i, j)$ and $P(j, i)$ to exchange the subvector $v_{i,*}$ and the subvector $v_{j,*}$. This gives the processor $P(i, j)$ access to (u, v) . It

follows that each processor $P(i, j)$ now has access to every entry in v corresponding to a nonzero in $L_{i,j}$. A similar procedure is previously implemented for distributed-memory breadth-first search [9].

Figure 2 illustrates an example with 1-based indexing, where $u = 1$ (red square in the leftmost matrix) is stored on process $P(1, 1)$ and $v = 12$ (green square) is stored on process $P(3, 4)$. If we assume that $P(1, 3)$ requires access to $v[1]$ and $v[12]$, an MPI_Allgather operation on the $P(1, :)$ row would provide access to $v[1]$, while the same operation on the $P(3, :)$ row would provide access to $v[12]$ on the transposed processor $P(3, 1)$. Point-to-point communication between $P(1, 3)$ and $P(3, 1)$ would then allow $P(1, 3)$ to access $v[12]$.

Once we have access to the processor assignment stored in v , we communicate edges to their target processor and build the local induced subgraph. To do this, we loop through each nonzero $(u, v) \in L_{i,j}$ stored on processor $P(i, j)$, and for each (u, v) where $v[u]$ and $v[v]$ are destined for the same destination processor, we construct a triple $(u, v, S(u, v))$ and place it on an outgoing buffer to the destination processor. A custom all-to-all ensures the required re-distribution of non-zeros. Once each processor has access to its edge set $E^{(P_i)}$, the local adjacency matrix of the induced subgraph is constructed; while we re-index the local matrix to fit its new, smaller size, we also keep a map of the original global vertex indices, since it is needed in the final phase.

Read Sequence Communication. The communication of read sequences is implemented separately, since the read sequences are not stored as nonzeros in the sparse matrix L , but in a distributed auxiliary data structure. Furthermore, a sequence is represented and stored as a char array. A large data set could exceed the MPI limit of $2^{31} - 1$. Therefore, we need to treat sequence communication separately and consider this potential limitation.

Read sequences that need to be sent to a processor other than the one they are currently on are packed into a char buffer and communicated as a sequence of non-blocking point-to-point messages in an all-to-all fashion. To deal with the MPI $2^{31} - 1$ count limit, we check the length of each message to be communicated and its receive buffer. If it goes beyond the limit, we communicate the sequences using a user-defined contiguous MPI data type whose size is equal to the buffer length. This way we can send and receive each character buffer in a single call.

4.4 Local Contig Assembly

Let $L_{i,j}$ be the local graph (or matrix), composed of one or more linear components, stored on the processor $P_{i,j}$ obtained via the induced subgraph algorithm. There are P such graphs, one for each processor, but we can assume without loss of generality that we are dealing only with $L(P_{i,j})$ or L for short.

Suppose L has n vertices and m edges. Each vertex of L is a read sequence l assigned by the partitioning algorithm to $P_{i,j}$. Then, we define $\Sigma = \{A, C, T, G\}$ as the alphabet of DNA nucleotides. Consequently, we represent the n sequences of L by $l_0, l_1, \dots, l_{n-1} \in \Sigma^*$, which means that each sequence is a combination of $\{A, C, T, G\}$. Given any read sequence l , we express the nucleotides of that sequence by $(l[0], l[1], \dots, l[|l| - 1])$, where $|l|$ denotes the length of the sequence. If $l[i]$ is a base or nucleotide in Σ , we denote the Watson-Crick complement base of $l[i]$ by $l[i]^c$. This allows us to generalize the notion of sequence to include its reverse complement,

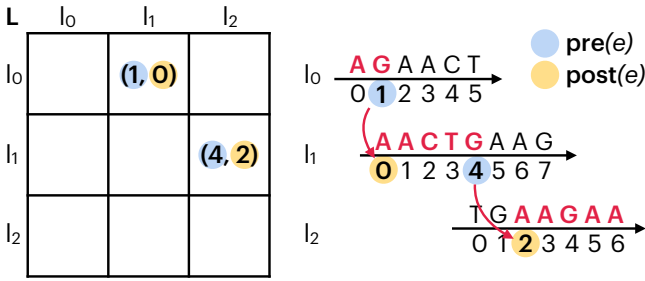


Figure 3: An example of how the local assembly algorithm concatenates sequences.

as defined in Section 2: if $i < j$, then we write $l[i : j]$ for the substring ($l[i], l[i + 1], \dots, l[j]$) and $l[j : i]$ for its reverse complement substring ($l[j]^c, [j - 1]^c, \dots, l[i]^c$).

L can also be viewed from the point of view of its matrix representation, such that L is a sparse ($n \times n$) matrix with m nonzeros. In the earlier stages of the pipeline, we use the doubly compressed sparse column (DCSC) format [8] to store our matrices for scalability. However, for the local traversal algorithm described in this section, we converted these matrices to compressed sparse column (CSC) format for simplicity and faster vertex (column) indexing. The storage space required to store the local matrices is an order of magnitude smaller than before and hence CSC does not introduce memory scalability issues despite hypersparsity. This conversion takes linear time in the number of local vertices, as only column pointers needs to be uncompressed and row indices array stays intact, and has negligible effect to overall runtime.

As a sparse matrix, $L(u, v) = e$ is a nonzero provided that the source sequence l_u and the destination sequence l_v overlap. In this nonzero e we store two values computed from the original string graph S , which is all we need for assembly: $\text{pre}_u(e)$ and $\text{post}_v(e)$. To define $\text{pre}_u(e)$ and $\text{post}_v(e)$, we use inclusive indexing, resulting in the following asymmetric definition. The first value $\text{pre}_u(e)$ stores the index i of l_u , which is the last nucleotide in l_u that does not overlap with l_v , i.e., the nucleotide on l_u that precedes the overlap with l_v . The second value $\text{post}_v(e)$ stores the index j of l_v , which is the first nucleotide in l_v that overlaps with l_u , i.e., the index of the beginning of the overlap between l_u and l_v . The definition is asymmetric because $l_u[i]$ and $l_v[j]$ do not store the same nucleotide. This asymmetry is necessary to compute the non-overlapping prefixes of each read in a contig, which, when joined together, produce a contig sequence.

For example, if $l_u = l_0 = AGAACT$ and $l_v = l_1 = AACTGAAG$ as shown in Figure 3 and we consider 0-based indexing, then $\text{pre}(e) = 1$ and $\text{post}(e) = 0$ because $l_u[2 : 5]$ and $l_v[0 : 3]$ overlap. If instead we consider $l_u = l_1 = AACTGAAG$ and $l_v = l_2 = TGAAGAA$, then $\text{pre}(e) = 4$ and $\text{post}(e) = 2$ because $l_u[5 : 7]$ and $l_v[2 : 4]$ overlap. It is also possible that $l_u = l_0$ would overlap with $l_v^c = l_1^c = CTTAGTT$ (the reverse complement of l_1). In this case, the same procedure would apply to compute $\text{pre}(e) = 1$ and $\text{post}(e) = 4$, where the overlapping subsequences would be $l_u[2 : 5]$ and $l_v^c[7 : 4]$, since the l_u subsequence $AACT$ would overlap with the l_v^c reserve complement subsequence $AGTT$.

Theoretically, the beginning of the overlapping substring of l_v should always be 0 or $|l_v| - 1$, depending on the orientation. Yet, we still store $\text{post}(e)$ because the diBELLA 2D [24] pipeline, which we extend in this work, uses an x-drop seed-and-extend approach to align overlapping sequences. With x-drop, the alignment between two sequences can potentially end early (i.e., before extending to the end of a read), leaving a short overhang in the alignment coordinates at the end of the sequence. If $l_u = l_1 = AACTGAAG$ and $l_v = l_2 = TGAAGAA$ are defined as in Figure 3, and the alignment told us that $l_u[5 : 7]$ and $l_v[2 : 4]$ were the overlapping region, it would be incorrect to match $\text{pre}(e) = 4$ with $\text{post}(e) = 0$, since we need $\text{post}(e) = 2$ to correctly concatenate the subsequences that form a contig. If we join the three partial sequences marked in red on l_0, l_1, l_2 in Figure 3, as explained below, we get a contig.

Because the local assembly operates directly on the CSC format, we describe it briefly. $L.JC$ is the column pointer array of length $n + 1$, $L.IR$ is the row index array of length m , and $L.VAL$ is the array of tuples $(\text{pre}(e), \text{post}(e))$, also of length m .

The local assembly algorithm is a variant of depth-first search, simplified by the fact that the maximum vertex degree of L is 2 by construction. For this reason, there is always only one vertex in the frontier, and the search is thus a linear walk. Each local matrix $L_{i,j}$ is assigned a contig set by multiway number partitioning, which is the set of connected components of $L_{i,j}$. Each vertex of L has degree 1 or 2. Moreover, we define contigs as linear chains of at least two sequences, where q is the number of vertices in a given connected component. It follows that any connected component consisting of $q \geq 2$ vertices must have exactly 2 vertices of degree 1 (i.e., *root* vertices) and $q - 2$ vertices of degree 2 (i.e., *intermediate* vertices). In short, the idea is to scan for root vertices in L and, if we find them, to take a walk from that root vertex (via as many intermediate vertices as necessary) until another root vertex is found. As we proceed, we perform the concatenation of subsequences described below. This search for the root vertex is performed over all n vertices. Therefore, we must mark each final root vertex (found by the linear traversal) as visited to avoid accidentally composing the same contig twice.

More precisely, we loop over the n sequence vertices in each subgraph $L_{i,j}$ and compute $L_{i,j}.JC[i + 1] - L_{i,j}.JC[i]$ from the column pointer array representing the degree of vertex i . Each time we find a vertex of degree 1, i.e., a root vertex, that has not been visited before, we perform a traversal starting from this that root vertex r . Given a generic vertex in the chain c (which can be either a root vertex or an intermediate vertex), we find the successor vertex c' by examining the vertices in the slice $L_{i,j}.IR[L_{i,j}.JC[c] : L_{i,j}.JC[c + 1]]$ of the row index array where the edges are stored. Each vertex c has at most two successor vertices, and we select the unvisited one. This process continues until we reach the vertex r' for which $L_{i,j}.JC[r' + 1] - L_{i,j}.JC[r'] = 1$, i.e., the second root vertex of a contig. The result is a chain of q vertices $r, c_1, \dots, c_{q-2}, r'$ for each contig stored in the submatrix $L_{i,j}$. As we proceed, we collect the edges between them e_0, e_1, \dots, e_{q-2} . Because the values for $\text{pre}(e_i)$ and $\text{post}(e_i)$ have already been computed and stored in each edge e_i , we know exactly which subsequences of which read sequence to look up and join to form the contig. Namely, $l_r[\alpha : \text{pre}(e_0)] \oplus l_{c_1}[\text{post}(e_0) : \text{pre}(e_1)] \oplus \dots \oplus l_{c_{q-2}}[\text{post}(e_{q-3}) :$

Table 1: Details of the machines used for evaluation; the frequency reported is the processor max turbo frequency.

Platform	Cores/Node	Frequency (GHz)	Processor	Memory (GB)	Network and Topology	L1	L2	L3
Cori Haswell	32	3.6	Intel Xeon E5-2698V3	128	Aries Dragonfly	64KB	256KB	40MB
Summit CPU	42	4.0	IBM POWER9	512	InfiniBand Non-Blocking Fat Tree	32KB	512KB	10MB

Table 2: Data sets used during evaluation: name, depth, number of sequences in the input, average read length, input size, genome size, and error rate.

Label	Depth	Reads (K)	Length	Input (GB)	Size (Mb)	Error (%)
O. sativa	30	638.2	19,695	12.2	500	0.5
C. elegans	40	420.7	14,550	3.8	100	0.5
H. sapiens	10	4,421.6	7,401	31.1	3,200	15.0

$\text{pre}(e_{q-2}) \oplus l_{c,r} [\text{post}(e_{q-2}) : \beta]$, where $\alpha = 0$ or $|l_r| - 1$ depending on the orientation of l_r , and β is similarly defined for l_r .

This algorithm is performed by each process in parallel on its own induced subgraph $L_{i,j}$. For each read in the contig, we either look for the subsequence in the locally stored char array that we started with, or in the char array obtained by communicating the read sequence. Because we store read sequences in large packed char arrays, we do not need to copy the entire read sequence to find the correct subsequence. Instead, we can simply use the offsets already computed, which tell us where each read is in the buffer, and then read the subsequence directly from the buffer. The algorithm is $O(q)$, where q is the number of vertices in a connected component as previously defined (i.e., the number of sequences in a contig), since the search for the root vertex takes linear time and the traversal is linear in the number of edges, which is $2(q - 1)$.

5 EXPERIMENTAL SETUP

To evaluate our contig generation algorithms and the ELBA long-read assembly pipeline we used two machines: the Haswell partition of the Cray XC40 supercomputer Cori at NERSC and the IBM supercomputer Summit at Oak Ridge National Laboratory, on which we used only IBM POWER9 CPUs (Table 1).

Each node on the Cori Haswell partition is a dual-socket 2.3GHz Intel Xeon with 16 cores each and 128GB of total memory, while each Summit node is a dual-socket IBM POWER9 with 22 cores each and 512GB of DDR4 from RAM, but only 42 cores are available because 2 of them are reserved for the operating system. On Cori Haswell, we used gcc-11.2 and the O3 flag to compile C/C++ codes, while on Summit we used gcc-9.2. On both machines, we used the default MPI implementation.

To evaluate our algorithm, we use three different species: *Oryza sativa* (O. sativa), *Caenorhabditis elegans* (C. elegans), and *Homo sapiens* (H. sapiens) whose characteristics are summarized in Table 2. The evaluation is divided into two categories: (a) runtime and scalability of the ELBA pipeline including our novel contig generation algorithm on two machines, and (b) runtime compared to state-of-the-art shared memory software. For low error rate sequences (O. sativa and C. elegans), we also report assembly quality.

The state-of-the-art software we consider are Hifiasm [11] and HiCanu [36], because of their speed and popularity, respectively, and both are written for shared-memory parallelism. HiCanu can

optionally run on grid computing, but is not implemented for distributed memory parallelism. It is worth noting that Hifiasm and HiCanu include additional polishing stages that make their overall assembly quality higher than ELBA’s. For the H. sapiens dataset, we consider Miniasm [30] and Canu [29], as this dataset has a much higher error rate that is not suitable for Hifiasm and HiCanu. Our goal is to show the competitiveness and potential of ELBA in terms of assembly quality, demonstrating in particular clear advantages in terms of runtime. ELBA was run with the k-mer length parameter $k = 31$ and the x-drop threshold $x = 15$ for the low error rate data and with $k = 17$ and $x = 7$ for H. sapiens in Table 2. Hifiasm and HiCanu were run with their default setting.

To show performance, we run ELBA on both Cori Haswell and Summit (except for H. sapiens, where we only use Summit), while for comparison with the state of the art, we only use Cori Haswell, since Hifiasm and HiCanu use SSE and AVX2 intrinsics, which are not supported on the IBM POWER9 processor on Summit. Hifiasm and HiCanu were developed for shared memory, so we only give runtimes for a single Cori Haswell node using multi-threading. The lack of support for AVX2 intrinsics is also the reason why ELBA’s alignment is slower on Summit than on Cori. For this reason, we want to emphasize that the goal of using two machines is to show performance and scaling on different systems, not to directly compare the two machines, since ELBA is optimized for a general HPC system, i.e., our code is general and no architecture-specific optimizations have been made.

To assess the quality of the contig set of ELBA, Hifiasm, and HiCanu, we use QUASt [25] and report the following metrics: Completeness, longest contig size, number of contigs, and misassembled contigs. Completeness measures the percentage of the reference genome to which at least one contig has been aligned. This is calculated by counting the number of nucleotides aligned to the reference genome and dividing by the total length. The number of misassembled contigs is defined as the number of contigs that contain incorrect assemblies, e.g., a contig consisting of sequences originating from different regions of the reference genome.

6 RESULTS

In this section, we evaluate the performance and quality of the overall ELBA pipeline and our novel contig generation algorithm, both individually and compared to the state of the art.

6.1 Performance and Scalability

Figure 4 illustrates the strong scaling of the entire ELBA pipeline for C. elegans on the left and for O. sativa on the right. The C. elegans dataset was run on $P = \{18, 32, 50, 72, 128\}$ nodes using 32 MPI ranks/nodes on both machines, while the O. sativa was run on $P = \{18, 32, 50, 72, 128\}$ nodes using 32 MPI ranks/nodes on Summit CPU and on $P = \{50, 72, 128\}$ nodes Cori Haswell because the algorithm

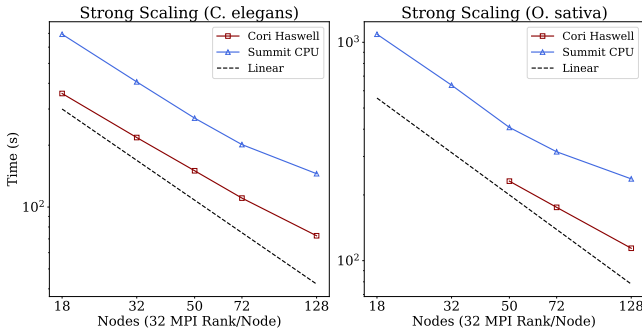


Figure 4: ELBA strong scaling on Cori Haswell and Summit CPU using 32 MPI rank/node on *C. elegans* (left) and on *O. sativa* (right).

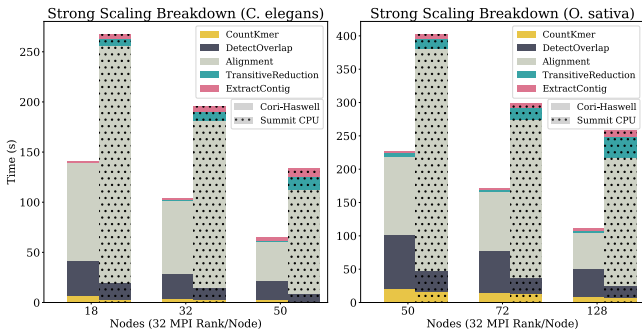


Figure 5: ELBA runtime breakdown of the main stages of the pipeline on Cori Haswell and Summit for *C. elegans* on the left and for *O. sativa* on the right.

for $P = \{18, 32\}$ ran out of memory since Cori Haswell has a smaller memory per node than Summit.

ELBA achieves a parallel efficiency of 75% on Cori Haswell and 69% Summit CPU for *C. elegans*, while it achieves a parallel efficiency of 80% and 64% for *O. sativa*. The parallel efficiency of *O. sativa* between 72 and 128 nodes on Summit is 83%, which is similar to the parallel efficiency on Cori between 50 and 128 nodes. For the *H. sapiens* dataset, the parallel efficiency on Summit between 200 and 392 nodes is close to 90%, as shown in Figure 6 on the left. These results show a good scaling behavior of the whole ELBA pipeline with a large input on two different architectures.

Figure 5 shows the runtime breakdown of ELBA on the two machines for *C. elegans* on the left and for *O. sativa* on the right, while Figure 6 on the right shows the runtime breakdown of ELBA on Summit for *H. sapiens*. To highlight the impact of the major stages, we omit I/O and other minor computation from the breakdown. The overall impact of the omitted computation is negligible.

The legend is arranged in reverse order with respect to the layers of the bar, i.e. the first entry of the legend at the top is associated with the first layer in the stacked bar from the bottom. CountKmer corresponds to the k-mer counting step, then follows the step DetectOverlap, which represents the time to create and compute the candidate overlap matrix C , i.e., the first step shown in Figure 1. Then comes the Alignment step, i.e., the time required to

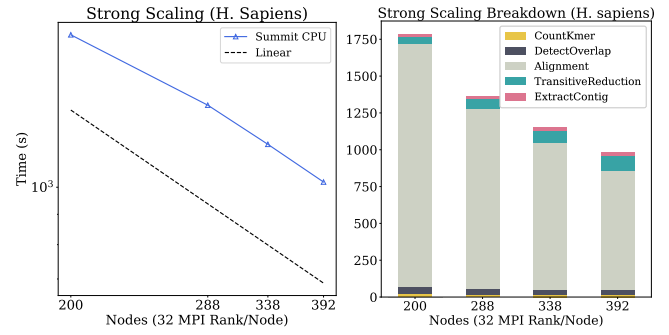


Figure 6: ELBA strong scaling (on the left) and runtime breakdown (on the right) of the main stages of the pipeline on Summit for *H. sapiens*.

perform pairwise alignment on each nonzero in the candidate overlap matrix C , followed by TrReduction, i.e., the transitive reduction time and the second step shown in Figure 1. Finally, ExtractContig is the time we spend extracting the contig set from the sparse matrix S and is shown as the third step in Figure 1. The ExtractContig step is the core contribution of this work, but its implementation is an essential part of making the entire ELBA pipeline work and for this reason it is key to showing the scalability of the pipeline.

Figure 5 shows the breakdown of ELBA performance for the main phases of computation for *C. elegans* and *O. sativa* using $P = \{50, 72, 128\}$ nodes on each machine while Figure 6 shows the breakdown of ELBA performance breakdown for *H. sapiens* using $P = \{200, 288, 338, 392\}$ Summit nodes. ELBA is faster overall on Cori Haswell than on Summit CPU. The CountKmer, DetectOverlap, and Alignment phases show nearly linear scaling on both machines, with the exception of CountKmer for *H. sapiens* on Summit, which scales only sublinearly. The relative contribution of pairwise alignment to the overall runtime increases on Summit CPU compared to Cori Haswell and largely contributes to the discrepancy in runtime because the alignment library used in ELBA is not optimized for the IBM processor. The TrReduction and ExtractContig phases are also significantly faster on Cori Haswell than on Summit CPU. On Summit, the computation for these two phases does not scale and consumes a higher percentage of runtime. This is because the amount of work is smaller in these two phases and the algorithms are latency-bound. Further, Summit's network has lower performance compared to Cori Haswell's. Summit CPU has lower network bandwidth per core, and we also only use 32 of the 42 available cores on Summit to make the comparison with Cori fair, which does not saturate Summit's bandwidth.

In each dataset, 65-85% of the runtime of contig generation on both machines is taken by the induced subgraph function described in Section 2, which mainly involves communication. The ExtractContig never requires more than 5% of the computation for each species and each machine, demonstrating the efficiency of our contig generation algorithm.

ELBA's contig generation focuses on localizing the graph traversal problem so that the sequences that make up a contig are organized into localized matrices on each processor. The working set at this stage is smaller than at the beginning of the computation, so the result is a fast and efficient, but latency-bound algorithm.

6.2 Comparison with the State-of-the-Art

To demonstrate the competitiveness and advantages of ELBA over state-of-the-art long read assembly software, we compare the runtime and scaling of ELBA with Hifiasm [11] and HiCanu [36] for *O. sativa* and *C. elegans* and with Mifiasm [30] and Canu [29] for *H. sapiens*. The competing software are designed for shared memory parallelism. Therefore, we ran them on a single Cori Haswell node with multithreading, while we ran ELBA on $P = \{18, 50, 128\}$ with 32 MPI ranks/nodes. Due to the hard-to-separate differences between these software, we decided to make a comparison based on total runtime. Hifiasm, HiCanu, Mifiasm, Canu, and ELBA perform very different computation, but they ultimately aim to solve the same problem. For the sake of completeness, we also compare the quality of assembly. It is worth noting that both Hifiasm and HiCanu perform a polishing phase. This can lead to a slight disadvantage in runtime, but ensures a better assembly quality.

Table 3 summarizes the runtime performance of Hifiasm and HiCanu, in the rightmost column the speedup of ELBA over those software for $P = \{18, 128\}$ and $P = \{50, 128\}$ for *C. elegans* and *O. sativa*, respectively. ELBA is up to 15× faster than Hifiasm and up to 58× faster than HiCanu for the *C. elegans* dataset, while the speedup for *O. sativa*, which is a larger genome, reaches 36× over Hifiasm and up to 159× over HiCanu. On Cori, runtimes for Hifiasm and HiCanu for *O. sativa* are 17 and 64 minutes, respectively, while ELBA takes less than 2 minutes on 128 nodes. For *C. elegans*, runtimes of Hifiasm and HiCanu are approximately 1 hour and 5 hours, while ELBA requires 1 minute on 128 nodes. For *H. sapiens*, ELBA on 392 nodes on Summit takes 17 minutes, while Mifiasm on Cori Haswell takes 1 hour and 30 minutes with 32 threads and Canu ran out of time after more than 64 hours of runtime with 32 threads on Cori Haswell. However, these times are from different architectures and are not directly comparable, so we do not give a speedup for *H. sapiens*. The results from *O. sativa* and *C. elegans* show that performance on Summit was worse than on Cori Haswell due to the less powerful processor on Summit.

Finally, we compare the quality of the assemblies of ELBA with that of Hifiasm and HiCanu. Table 4 summarizes metrics obtained from QUAST [25]. Specifically, we show the completeness, i.e., the proportion of the reference genome that was covered by at least one contig (the higher, the better), then the length of the longest contig (the higher, the better), the size of the contig set (the lower, the better if associated with high completeness), and the number of misassemblies (the lower, the better). In both species, ELBA has competitive genome completeness, especially in *C. elegans*, where it is higher than both Hifiasm and HiCanu, and misassemblies. In ELBA, the contigs are significantly shorter than in the two competing software. This is understandable, since ELBA does not currently perform a polishing step, which is reserved as future work.

7 CONCLUSIONS

Recent advances in sequencing technologies have increased the need for high-performance approaches, as we can now generate more data at lower cost, which in turn requires higher computational resources to reconstruct high-quality assemblies in a timely manner. In this paper, we presented the contig generation phase of the distributed-memory long-read assembler ELBA.

Table 3: ELBA’s speedup over state-of-the-art software. Hifiasm and HiCanu are designed for shared memory parallelism and were run on a single Cori node with multithreading.

Tool	Organism	Runtime (s)	Nodes (32 MPI Rank/Node)	ELBA Speed-Up
Hifiasm	<i>C. elegans</i>	1,015.2	18–128	3–15×
HiCanu	<i>C. elegans</i>	3,819.0	18–128	11–58×
Hifiasm	<i>O. sativa</i>	4,131.9	50–128	18–36×
HiCanu	<i>O. sativa</i>	18,131.0	50–128	78–159×

Table 4: Comparison of assembler quality for *O. sativa* (top) and *C. elegans* (bottom). Hifiasm and HiCanu implement additional polishing stages to improve their metrics.

Tool	Completeness (%)	Longest Contig (Mb)	Contigs	Misassembled Contigs
ELBA	37.09	0.172	6411	2
Hifiasm	26.94	7.083	1661	1
HiCanu	25.94	37.523	168	2
ELBA	98.93	0.313	4287	5
Hifiasm	99.96	6.438	133	0
HiCanu	99.90	18.332	32	2

Contig generation is critical to assembly functionality, as it enables the construction of longer genomic sequences that represent a physical map of a region of a chromosome. ELBA has achieved speed increases of up to 36× and 159× compared to two state-of-the-art software for the *O. sativa* dataset, opening the door for high-performance genome assembly.

ELBA and its contig generation step rely on distributed sparse matrices to first determine the contig set starting from a string graph. Then, using a greedy multiway number partitioning algorithm, it determines how the rows and columns of the sparse matrix representing DNA sequences are redistributed between processes so that sequences belonging to the same contig are stored locally on the same processor. ELBA then uses such partitioning and the sparse matrix abstraction to implement the induced subgraph function and redistribute the sequences among the processes. Finally, ELBA’s contig generation step computes a local assembly step, i.e., the actual concatenation of sequences into a contig, on each processor independently and in parallel.

Future work includes developing a polishing or scaffolding phase to further improve the quality of ELBA assembly. One possibility is to once again use the sparse matrix abstraction to find similarities within the contig set and obtain even longer sequences. In addition, we plan to reduce the memory consumption of ELBA so that we can assemble large genomes at low concurrency, and optimize ELBA for running in a cloud environment as high-performance scientific computing in the cloud becomes more popular [22, 32, 38]. Finally, we plan to use GPUs in several stages, such as alignment [1, 41] and k-mer counting [15, 35], to improve our performance and take full advantage of today’s heterogeneous systems.

ACKNOWLEDGMENTS

This work is supported by the Advanced Scientific Computing Research program within the Office of Science of the DOE under contract number DE-AC02-05CH11231, and by the Exascale Computing Project (17-SC-20-SC), a collaborative effort of the DOE Office of Science and the NNSA. We used resources of the NERSC supported by the Office of Science of the DOE under Contract No.

DEAC02-05CH11231 and of the OLCF supported by the Office of Science of the DOE under Contract No. DE-AC05-00OR22725.

REFERENCES

- [1] Muaaz G Awan, Jack Deslippe, Aydın Buluç, Oguz Selvitopi, Steven Hofmeyr, Leonid Oliker, and Katherine Yelick. 2020. ADEPT: a domain independent sequence alignment strategy for GPU architectures. *BMC Bioinformatics* 21, 1 (2020), 1–29.
- [2] Baruch Awerbuch and Yossi Shiloach. 1987. New connectivity and MSF algorithms for shuffle-exchange network and PRAM. *IEEE Trans. Comput.* 36, 10 (1987), 1258–1263.
- [3] Ariful Azad and Aydın Buluç. 2019. LACC: A Linear-Algebraic Algorithm for Finding Connected Components in Distributed Memory. In *IEEE International Parallel and Distributed Processing Symposium (IPDPS)*. ACM New York, NY, USA.
- [4] Ariful Azad, Oguz Selvitopi, Md Taufique Hussain, John R. Gilbert, and Aydın Buluç. 2022. Combinatorial BLAS 2.0: Scaling Combinatorial Algorithms on Distributed-Memory Systems. *IEEE Transactions on Parallel & Distributed Systems* 33, 4 (2022), 989–1001. <https://doi.org/10.1109/TPDS.2021.3094091>
- [5] John Bachan, Scott B. Baden, Steven Hofmeyr, Mathias Jacquelin, Amir Kamil, Dan Bonachea, Paul H. Hargrove, and Hadia Ahmed. 2019. UPC++: A High-Performance Communication Framework for Asynchronous Computation. In *33rd IEEE International Parallel and Distributed Processing Symposium (IPDPS'19)* (Rio de Janeiro, Brazil). IEEE. <https://doi.org/10.25344/S4V88H>
- [6] Konstantin Berlin, Sergey Koren, Chen-Shan Chin, James P Drake, Jane M Landolin, and Adam M Phillippy. 2015. Assembling large genomes with single-molecule sequencing and locality-sensitive hashing. *Nature Biotechnology* 33, 6 (2015), 623–630.
- [7] Maciej Besta, Raghavendra Kanakagiri, Harun Mustafa, Mikhail Karasikov, Gunnar Rätsch, Torsten Hoefler, and Edgar Solomonik. 2020. Communication-efficient jaccard similarity for high-performance distributed genome comparisons. In *International Parallel and Distributed Processing Symposium (IPDPS)*. IEEE, IEEE Computer Society, 1122–1132.
- [8] Aydın Buluç and John R Gilbert. 2008. On the representation and multiplication of hypersparse matrices. In *2008 IEEE International Symposium on Parallel and Distributed Processing*. IEEE, 1–11.
- [9] Aydın Buluç and Kamesh Madduri. 2011. Parallel breadth-first search on distributed memory systems. In *Proceedings of International Conference for High Performance Computing, Networking, Storage and Analysis (SC)*. 1–12.
- [10] William W Carlson, Jesse M Draper, David E Culler, Kathy Yelick, Eugene Brooks, and Karen Warren. 1999. *Introduction to UPC and language specification*. Technical Report. Technical Report CCS-TR-99-157, IDA Center for Computing Sciences.
- [11] Haoyu Cheng, Gregory T Concepcion, Xiaowen Feng, Haowen Zhang, and Heng Li. 2021. Haplotype-resolved de novo assembly using phased assembly graphs with hifiasm. *Nature methods* 18, 2 (2021), 170–175.
- [12] Chen-Shan Chin, Paul Peluso, Fritz J Sedlazeck, Maria Nattestad, Gregory T Concepcion, Alicia Clum, Christopher Dunn, Ronan O'Malley, Rosa Figueroa-Balderas, Abraham Morales-Cruz, et al. 2016. Phased diploid genome assembly with single-molecule real-time sequencing. *Nature methods* 13, 12 (2016), 1050–1054.
- [13] Jack Edmonds and Ellis L Johnson. 2003. Matching: A well-solved class of integer linear programs. In *Combinatorial Optimization—Eureka, You Shrink!* Springer, 27–30.
- [14] John Eid, Adrian Fehr, Jeremy Gray, Khai Luong, John Lyle, Geoff Otto, Paul Peluso, David Rank, Primo Baybayan, Brad Bettman, et al. 2009. Real-time DNA sequencing from single polymerase molecules. *Science* 323, 5910 (2009), 133–138.
- [15] Marius Erbert, Steffen Rechner, and Matthias Müller-Hannemann. 2017. Gerbil: a fast and memory-efficient k-mer counter with GPU-support. *Algorithms for Molecular Biology* 12, 1 (2017), 1–12.
- [16] Evangelos Georganas, Aydın Buluç, Jarrod Chapman, Steven Hofmeyr, Chaitanya Aluru, Rob Egan, Leonid Oliker, Daniel Rokhsar, and Katherine Yelick. 2015. HipMer: an extreme-scale de novo genome assembler. In *The International Conference for High Performance Computing, Networking, Storage and Analysis (SC)*. ACM, ACM, New York, NY, 14.
- [17] Evangelos Georganas, Rob Egan, Steven Hofmeyr, Eugene Goltsman, Bill Arndt, Andrew Tritt, Aydın Buluç, Leonid Oliker, and Katherine Yelick. 2018. Extreme scale de novo metagenome assembly. In *SC18: International Conference for High Performance Computing, Networking, Storage and Analysis*. IEEE, IEEE Computer Society, 122–134.
- [18] Priyanka Ghosh, Sriram Krishnamoorthy, and Ananth Kalyanaraman. 2020. PaKMan: A Scalable Algorithm for Generating Genomic Contigs on Distributed Memory Machines. *IEEE Transactions on Parallel and Distributed Systems* 32, 5 (2020), 1191–1209.
- [19] Sara Goodwin, James Gurtowski, Scott Ethe-Sayers, Panchajanya Deshpande, Michael C Schatz, and W Richard McCombie. 2015. Oxford Nanopore sequencing, hybrid error correction, and de novo assembly of a eukaryotic genome. *Genome Research* 25, 11 (2015), 1750–1756.
- [20] Ronald L Graham. 1966. Bounds for certain multiprocessing anomalies. *Bell system technical journal* 45, 9 (1966), 1563–1581.
- [21] Ronald L. Graham. 1969. Bounds on multiprocessing timing anomalies. *SIAM journal on Applied Mathematics* 17, 2 (1969), 416–429.
- [22] Giulia Guidi, Marquita Ellis, Aydın Buluç, Katherine Yelick, and David Culler. 2021. 10 years later: Cloud computing is closing the performance gap. In *Companion of the ACM/SPEC International Conference on Performance Engineering*. 41–48.
- [23] Giulia Guidi, Marquita Ellis, Daniel Rokhsar, Katherine Yelick, and Aydın Buluç. 2021. BELLA: Berkeley efficient long-read to long-read aligner and overlapper. In *SIAM Conference on Applied and Computational Discrete Algorithms (ACDA21)*. SIAM, SIAM, 123–134.
- [24] Giulia Guidi, Oguz Selvitopi, Marquita Ellis, Leonid Oliker, Katherine Yelick, and Aydın Buluç. 2021. Parallel string graph construction and transitive reduction for de novo genome assembly. In *IEEE International Parallel and Distributed Processing Symposium (IPDPS)*. IEEE, IEEE Computer Society, 517–526.
- [25] Alexey Gurevich, Vladislav Saveliev, Nikolay Vyahhi, and Glenn Tesler. 2013. QUAST: quality assessment tool for genome assemblies. *Bioinformatics* 29, 8 (2013), 1072–1075.
- [26] Steven Hofmeyr, Rob Egan, Evangelos Georganas, Alex C Copeland, Robert Riley, Alicia Clum, Emiley Eloie-Fadrosh, Simon Roux, Eugene Goltsman, Aydın Buluç, et al. 2020. Terabase-scale metagenome coassembly with MetaHipMer. *Scientific reports* 10, 1 (2020), 1–11.
- [27] Ting Hon, Kristin Mars, Greg Young, Yu-Chih Tsai, Joseph W Karalius, Jane M Landolin, Nicholas Maurer, David Kudrna, Michael A Hardigan, Cynthia C Steiner, et al. 2020. Highly accurate long-read HiFi sequencing data for five complex genomes. *Scientific data* 7, 1 (2020), 1–11.
- [28] Mikhail Kolmogorov, Jeffrey Yuan, Yu Lin, and Pavel A Pevzner. 2019. Assembly of long, error-prone reads using repeat graphs. *Nature biotechnology* 37, 5 (2019), 540–546.
- [29] Sergey Koren, Brian P Walenz, Konstantin Berlin, Jason R Miller, Nicholas H Bergman, and Adam M Phillippy. 2017. Canu: scalable and accurate long-read assembly via adaptive k-mer weighting and repeat separation. *Genome research* 27, 5 (2017), 722–736.
- [30] Heng Li. 2016. Minimap and miniasm: fast mapping and de novo assembly for noisy long sequences. *Bioinformatics* 32, 14 (2016), 2103–2110.
- [31] Paul Medvedev, Konstantinos Georgiou, Gene Myers, and Michael Brudno. 2007. Computability of models for sequence assembly. In *International Workshop on Algorithms in Bioinformatics*. Springer, 289–301.
- [32] Olivier Mesnard and Lorena A Barba. 2019. Reproducible workflow on a public cloud for computational fluid dynamics. *Computing in Science & Engineering* 22, 1 (2019), 102–116.
- [33] Jason R Miller, Arthur L Delcher, Sergey Koren, Eli Venter, Brian P Walenz, Anushka Brownley, Justin Johnson, Kelvin Li, Clark Mobarry, and Granger Sutton. 2008. Aggressive assembly of pyrosequencing reads with mates. *Bioinformatics* 24, 24 (2008), 2818–2824.
- [34] Niranjana Nagarajan and Mihai Pop. 2009. Parametric complexity of sequence assembly: theory and applications to next generation sequencing. *Journal of Computational Biology* 16, 7 (2009), 897–908.
- [35] Israt Nisa, Prashant Pandey, Marquita Ellis, Leonid Oliker, Aydın Buluç, and Katherine Yelick. 2021. Distributed-Memory k-mer Counting on GPUs. In *IEEE International Parallel and Distributed Processing Symposium (IPDPS)*. IEEE, 527–536.
- [36] Sergey Nurk, Brian P Walenz, Arang Rhee, Mitchell R Vollger, Glennis A Logsdon, Robert Grothe, Karen H Miga, Evan E Eichler, Adam M Phillippy, and Sergey Koren. 2020. HiCanu: accurate assembly of segmental duplications, satellites, and allelic variants from high-fidelity long reads. *Genome research* 30, 9 (2020), 1291–1305.
- [37] Adam M Phillippy, Michael C Schatz, and Mihai Pop. 2008. Genome assembly forensics: finding the elusive mis-assembly. *Genome Biology* 9, 3 (2008), R55.
- [38] Daniel Reed, Dennis Gannon, and Jack Dongarra. 2022. Reinventing High Performance Computing: Challenges and Opportunities. *arXiv preprint arXiv:2203.02544* (2022).
- [39] Oguz Selvitopi, Saliya Ekanayake, Giulia Guidi, Georgios Pavlopoulos, Ariful Azad, and Aydın Buluç. 2020. Distributed Many-to-Many Protein Sequence Alignment Using Sparse Matrices. *The International Conference for High Performance Computing, Networking, Storage and Analysis (SC)* (2020).
- [40] Kishwar Shafin, Trevor Pesout, Ryan Lorig-Roach, Marina Haukness, Hugh E Olsen, Colleen Bosworth, Joel Armstrong, Kristof Tigyi, Nicholas Maurer, Sergey Koren, et al. 2020. Nanopore sequencing and the Shasta toolkit enable efficient de novo assembly of eleven human genomes. *Nature biotechnology* 38, 9 (2020), 1044–1053.
- [41] Alberto Zeni, Giulia Guidi, Marquita Ellis, Nan Ding, Marco D Santambrogio, Steven Hofmeyr, Aydın Buluç, Leonid Oliker, and Katherine Yelick. 2020. LOGAN: High-performance GPU-based X-drop long-read alignment. In *International Parallel and Distributed Processing Symposium (IPDPS)*. IEEE, 462–471.
- [42] Wenyu Zhang, Jiajia Chen, Yang Yang, Yifei Tang, Jing Shang, and Bairong Shen. 2011. A practical comparison of de novo genome assembly software tools for next-generation sequencing technologies. *PLoS One* 6, 3 (2011), e17915.